INTIAL STATE RADIATION AND INCLUSIVE HADRON PRODUCTION MEASUREMENTS AT BABAR.

F. ANULLI

University of Perugia and Laboratori Nazionali di Frascati dell'INFN,
via E.Fermi 40, I-00044 Frascati (Rm), Italy

The status of analysis of processes with hard photon emitted from the initial state (ISR) at *BABAR* is presented. We tag events by the presence of a hard photon in the detector, then reconstruct $\mu^+\mu^-$ and several excxusive hadronic final states. The invariant mass of the final state determines an effective collision center of mass energy at which these measurements can be compared with results from direct e^+e^- annihilation process. The first results on $e^+e^- \to 2h^+2h^-$, where $h = \pi, K$ and on $e^+e^- \to J/\psi$, obtained with a sample of 89.3 fb^{-1}, are presented.

Measurements of inclusive η, π^+, K^+ and $p/\bar{p}$ production cross sections below the $\Upsilon(4S)$ resonance are also presented. These measurements have nearly complete momentum coverage and precision comparable to the best measurements at higher energies. They therefore allow for precise tests of QCD predictions and fragmentation models at 10.54 GeV and of their scaling properties.

1 Initial State Radiation processes at *BABAR*.

Initial state radiation (ISR) processes can be effectively used to measure e^+e^- annihilation at high luminosity e^+e^- storage rings, such as the *B-factory* PEP-II [1,2,3]. A large mass range is accessible in a single experiment, contrary to the case with fixed energy colliders, which are optimized only in a limited region. In addition, the broad-band coverage may result also in greater control of systematic effects because only one experimental setup is involved.

The ISR physics program consists mainly on light hadron spectroscopy and measurement of the ratio R $= \sigma(e^+e^- \to \text{h}adrons)/\sigma(e^+e^- \to \mu^+\mu^-)$, which provides the experimental input to dispersion integrals for computation of the hadronic contribution to the theoretical estimation of the muon magnetic moment anomaly, $a_\mu = (g-2)_\mu/2$ and of the running of the electromagnetic coupling to the Z pole, $\alpha(M_Z^2)$.

The ISR cross section for a particular final state f is related to the cross section for the direct annihilation $e^+e^- \to f$ through

$$\frac{d\sigma(s,x)}{dx} = W(s,x)\,\sigma_f(s'), \qquad s' = s(1-x); \qquad (1)$$

where $x = 2E_\gamma^\star/\sqrt{s}$, $E_\gamma^\star$ is the radiated photon energy in the nominal center-of-mass frame and $\sqrt{s}$ the nominal c.m. energy of the collider. The quantity $s' = s(1-x)$ represents the mass squared of the final state system, f. The radiator function $W(s,x)$ describes the virtual photon energy spectrum and can be computed to an accurcy better than 1%. The direction of radiated photon is peaked along the initial beams, but for $\sqrt{s} \simeq 10$ GeV the fraction at large angle is
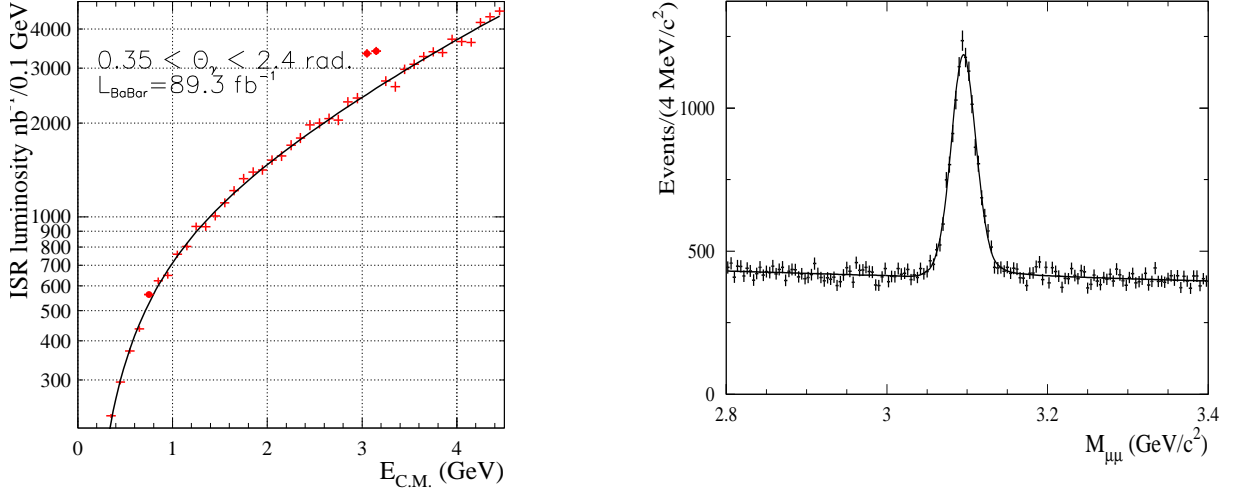
Figure 1: Left: measured ISR luminosity, integrated over 0.1 GeV for 89.3 fb^{-1} of $BABAR$ integrated luminosity. On the right: the reconstructed $\mu^+\mu^-$ invariant mass distribution in the J/ψ region.

relatively large. It has been shown a 10-15% acceptance for these photons in $BABAR$. The measurement of the corresponding leptonic process $e^+e^- \to \mu^+\mu^-\gamma$ provides the ISR luminosity. Thus, the Born cross section for a hadronic final state $\sigma_f(s')$ is given by

$$\sigma_f(s') \;=\; \frac{\Delta N_{f\gamma}\ \epsilon_{\mu\mu}\ (1 + \delta_{FSR}^{\mu\mu})}{\Delta N_{\mu\mu\gamma}\ \epsilon_f\ (1 + \delta_{FSR}^f)}\ \sigma_{\mu\mu}(s') \tag{2}$$

where $\Delta N_{f\gamma}$ ($\Delta N_{\mu\mu\gamma}$) are the number of detected $f\gamma$ ($\mu\mu\gamma$) events in the bin of width $\Delta s'$ centered at s'. ϵ_f ($\epsilon_{\mu\mu}$) and δ_{FSR}^f ($\delta_{FSR}^{\mu\mu}$) are respectively the detection efficiencies and fractions of events when the hard photon is emitted by final-state particles. The latter quantity can be sizable for the $\mu\mu$ channel, but negligible for most of the low energy hadronic states, which have vanishingly small cross sections at the nominal machine energy.

1.1 The di-muon final state and ISR luminosity at BABAR

The data used in the analysis presented here correspond to an integrated luminosity of $89.3\,\mathrm{fb}^{-1}$ collected both at the $\Upsilon(4S)$ and in the nearby continuum, with the $BABAR$ detector at the PEP-II asymmetric B-factory.

The $BABAR$ detector is described elsewhere [4]. The information from the tracking system (Silicon Vertex Tracker and Drift Chamber) is used to measure angles and momenta of charged particles. The quartz Cherenkov radiator (DIRC) is the main subsystem for particle identification (K/π separation is an essential ingredient for these studies). Muons are identified in the Resistive Plate Counters installed in the magnet yoke of the $BABAR$ solenoid, while photons are detected in the CsI calorimeter.

Events are tagged by detecting a photon with an energy in the c.m. system larger than 3 GeV. The invariant mass of the dimuon system determines the effective collision energy. A disadvantage deriving from the use of ISR events is the invaraiant mass resolution, comparing to the case of fixed energy machines. The resolution can be improved by a kinematics fit constraining the mass recoiling against the reconstructed final state to be equal to zero, that is the photon mass. After the kinematics fit the invariant mass resolution improves from 16 MeV/c^2 to 8 MeV/c^2 at the J/ψ mass. In addition the fit effectively removes background from $\tau^+\tau^-$ events. Fig. 1(left) show the derived spectrum of ISR luminosity per 100 MeV energy bins. The $BABAR$ luminosity
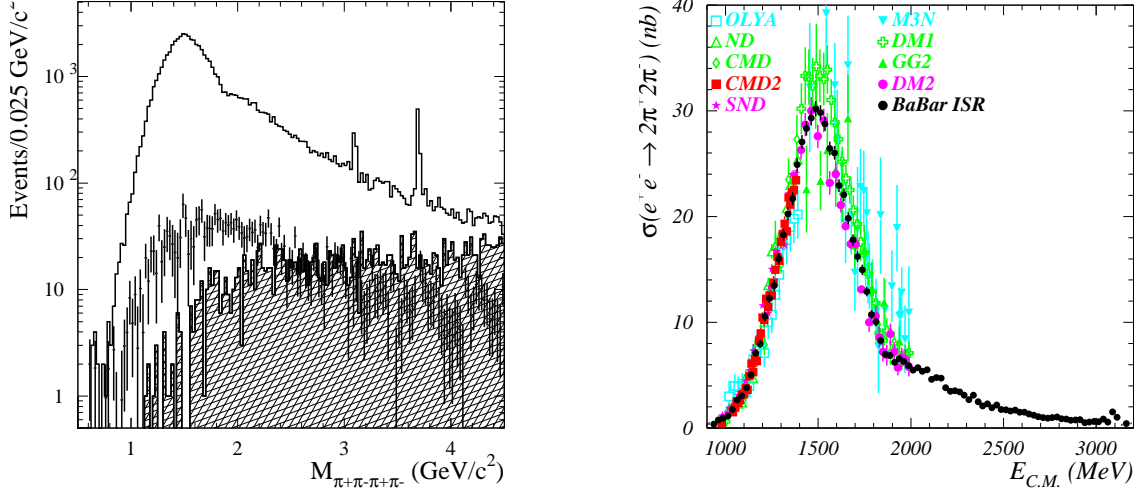
Figure 2: Left: the four-pion invariant mass distribution. The points indicate the estiimated ISR-type backgrund, while the cross-hatched histogram corresponds to the non-ISR background. On the right: $e^+e^- \to 2\pi^+2\pi^-$ cross section as a function of energy obtained with $BABAR$ ISR data (black dots) in comparison with all previous e^+e^- data.

of 89 fb^{-1} is equivalent to an e^+e^- machine energy scan in steps of 0.1 GeV, with a luminosity integral per point varying from 0.7 pb^{-1} at 1 GeV up to 3.6 pb^{-1} at 4 GeV. This luminosity integral provides already a statistically competitive hadron sample, especially in the energy range between 1.4 and 3.5 GeV, where very few data are presently available. The systematic error is estimated to be of the order of 3%(5% for energies below 1 GeV).

1.2 Hadronic channels

A very rich program can be exploited in $BABAR$ from the study of hadronic final states: spectroscopy, form factor measurements, search for exotic states, etc. Besides, measurements of exclusive hadronic channels constitute the main approach for measuring R. Currently the major hadronic final states are under study ($\pi\pi, KK, 4\pi, 5\pi, 6\pi, 2K2\pi, 4K, p\bar{p}, KK\pi$) and more are planned.

Preliminary results are available for the final states with four charged hadrons, namely $2\pi^+2\pi^-$, $2K^+2K^-$, $K^+K^-\pi^+\pi^-$. The discrimination between the three final states is done on the basis of the particle identification and on the kinematics fit results for the different mass hypothesis.

No muon identification was applied since no corresponding background is expected in this sample. The background from other hadronic channels is small and is subtracted in each mass bin. Overall, more than 70000 events have been selected leading to small statistical uncertainties. The estimated systematic error is about 5% in the energy region between 1 and 3 GeV, dominated by the luminosity determination. Fig. 2(right) shows the derived cross section for the 4 pions channel in 25 MeV steps. $BABAR$ data are in good agreement with previous available results. Moreover, $BABAR$ is the only experiment which cover the entire energy range, with an accuracy comparable to the latest precise results from CMD-2 [5] and SND [6] below 1.4 GeV, and much better accuracy than older results from DCI and ADONE above 1.4 GeV.

The hadronic contribution for this particular channel evaluated using all available e^+e^- data in 0.56-1.8 GeV energy range is [8] $a_\mu^{hadr} = (14.21 \pm 0.87_{exp} \pm 0.23_{rad})10^{-10}$, while the τ data give $a_\mu^{hadr} = (12.35 \pm 0.96_{exp} \pm 0.40_{SU2})10^{-10}$. The $BABAR$ data in the same energy region give instead [7] $a_\mu^{hadr} = (12.95 \pm 0.64_{exp} \pm 0.13_{rad})10^{-10}$, leading to a substantial improvement.

1.3 Measurement of J/ψ width

For a narrow state of mass M such as J/ψ, decaying into a final state f, the Breit-Wigner can be approximated by a δ function and the production cross section can be written as:

$$\sigma_{e^+e^- \to J/\psi\gamma \to f\gamma} = \frac{12\pi^2\Gamma_{ee}B_f}{Ms} \, W(s, x_0); \tag{3}$$

where $x_0 = 1 - M^2/s$. The ratio of $\mu^+\mu^-$ events from J/ψ peak (about 7800 events observed in $89\,\mathrm{fb}^{-1}$, fig. 1(right)) to the continuum allows to extract the product [9]

$$\Gamma(J/\psi \to e^+e^-) \, B_{J/\psi \to \mu^+\mu^-} = (0.330 \pm 0.008_{stat} \pm 0.007_{syst})\mathrm{keV}. \tag{4}$$

Background estimation, J/ψ line shape, radiative corrections and Monte Carlo statistics constitute the main contributions to the systematic error. Using the world average values for the branching fraction $B_{J/\psi \to \mu^+\mu^-}$ and $B_{J/\psi \to e^+e^-}$, we derive the J/ψ electronic and total widths, $\Gamma_{J/\psi \to e^+e^-} = (5.61 \pm 0.20)$ keV and $\Gamma_{J/\psi} = (94.7 \pm 4.4)$ keV, which represent an improvement with respect to the present world average values of respectively (5.26 ± 0.37) keV and (87 ± 5) keV.

2 Inclusive hadron production studies

BABAR has performed measurements of inclusive production cross sections and fractions of etas and charged pions, kaons and protons, both from $\Upsilon(4S)$ decays and in continuum (at $E_{CM} = 10.54$ GeV, below the $B\text{-}\bar{B}$ production threshold). The quark-antiquark colorless system created in the continuum events "fragments" into a number of primary hadrons, which then decay into stable hadrons. The fragmentation process has been extensively studied at higher energies, in particular in the Z^0 region and a number of models have been developped and tested.

Models have been tuned for high energies, but fundamental tests, such as the study of scaling properties, need accurate inclusive measurement of hadron productions also at lower energies. Previous measurements performed at Argus and Cleo at an energy of ~ 10 GeV were not able to cover the full kinematics range. *BABAR* data are consistent with those results and extend coverage up to the highest momentum values with an accuracy at few percent level.

Fig. 3 shows the differential cross sections in continuum events for π, K and $p(\bar{p})$ as a function
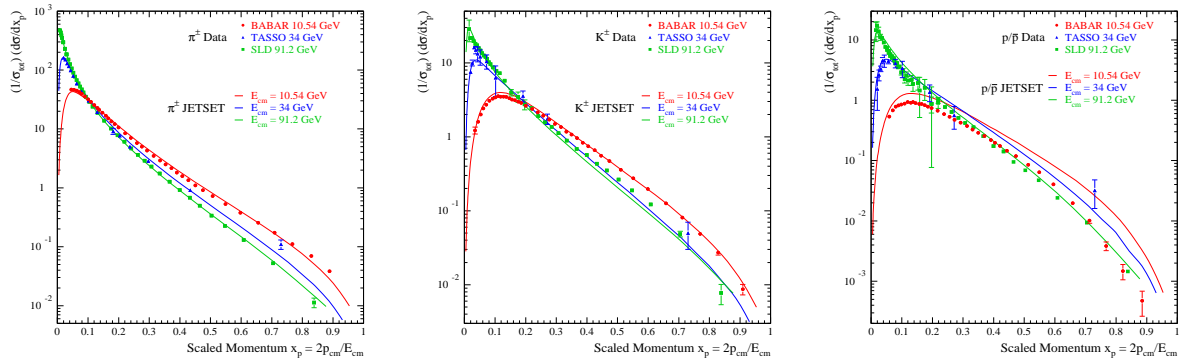

Figure 3: Differential pion (left), kaon (middle) and proton (right) cross section from continuum data in *BABAR* (red points), compared with results by TASSO at c.m. energy of 34 GeV (blu triangles) and by SLD at 91.2 GeV (green squares). Predictions by JETSET Monte Carlo for different energies are superimposed with corresponding color code.

of x_p, the momentum scaled by half of the center-of-mass energy. *BABAR* data, obatined from

a sample of 0.9 fb^{-1}, are shown along with those from experiment at higher energies, namely TASSO [11] at 34 GeV and SLD [12] at 91.2 GeV. The nearly full kinematics range coverage and the comparable precision between $BABAR$ and SLD data, allow to study scaling properties of hadronization and to test the predictions by the various fragmentation models. Hadronization should be scale invariant. Therefore, cross sections are expected to differ only because of small scaling violation effects. At low x_p the difference is due to the mass of the hadrons, with a cut-off at $x_p \simeq 2m_h/E_{CM}$. At high momentum, substantial scaling violation is expected because of running of α_s, as it is indeed observed for pions cross-sections. This behavior for pions is well reproduced by most of the fragmentation models, as shown for the case of JETSET [13] in the same fig. 3(left). A similar behavior is expected also for the others hadrons, but the data show little scaling violation for kaons, and almost no violation for protons. These results, even if preliminary, represent already very useful inputs for tuning the simulation of fragmentation processes down to an energy of 10 GeV.

2.1 Test of QCD predictions in the MLLA model

These data can also be used to test some predictions of QCD in the Modified Leading Logarithm Approximation (MLLA) [14]. For this purpose, it is convenient to plot the differential cross section as a function of the variable $\xi = -\ln(x_p)$. MLLA predicts that a slightly distorted gaussian function should be able to fit the data over almost the full kinematic range. Fig. 4 show the distributions for π, K, η and $p/\bar{p}$ with the results of the fit. The distorted Gaussian is able to describe the $BABAR$ data at the few percent level over the full measured momentum region with reasonably small skewness and kurtosis values, consistent with theoretical predictions.
The position of the peak $\xi^\star$ of the ξ distribution is predicted to decrease exponentially with increasing particle mass. The $\xi^\star$ values reported in table 1 show a clear disagreement with this prediction: the value for pions is quite different from the others, but those for protons and kaons are very similar one another, then inconsistent with a continued exponential decrease. This qualitative behavior is not peculiar of the $BABAR$ operational energy region, but it has been already observed at higher energies and it is particularly evident in measurements performed at ~ 90 GeV.

Table 1: Position of the peaks $\xi^\star$ of the ξ distributions for π, k, η and $p(\bar{p})$.

particle type	$\xi^\star$
π^+	2.36 $\pm$ 0.01
K^+	1.64 $\pm$ 0.01
η	1.44 $\pm$ 0.02
$p(\bar{p})$	1.61 $\pm$ 0.01

3 Conclusions

Preliminary results from $BABAR$ on final states produced through ISR demonstrate the high physics potential of this sample, which should yield precise measurements of e^+e^- annihiliation cross sections. The ratio R $= \sigma(e^+e^- \to \mathrm{h}adrons)/\sigma(e^+e^- \to \mu^+\mu^-)$, will be measured from the sum of exclusive channels, providing input for theoretical determination of the hadronic contribution to $(g-2)_\mu$ and $\alpha(M_Z^2)$. The preliminary $e^+e^- \to 2\pi^+2\pi^-$ cross section, from threshold up to 4.5 GeV has been obtained, with a systematic error of about 5% in the central region. The radiative return to J/ψ resonance allows to measure the relative branching fractions
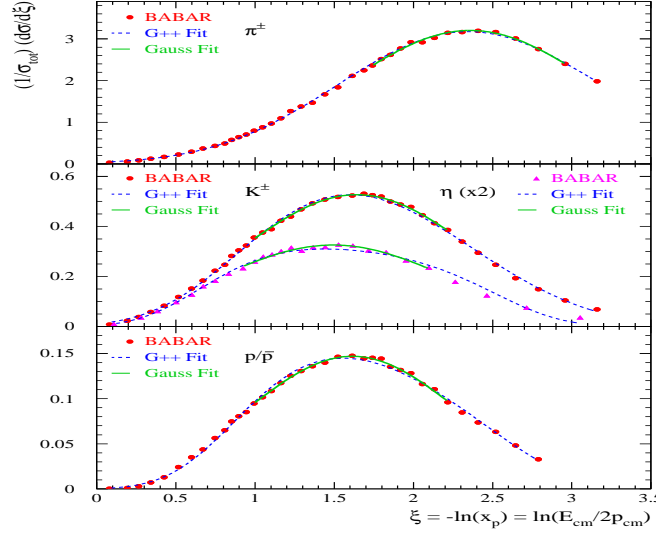
Figure 4: Differential pion (top), kaon, eta (middle) and proton (bottom) cross section in the continuum data (solid symbols) as a function of $\xi = -\ln(x_p)$ shown with the result of a Gaussian fit to the data (solid lines) and of a distorted Gaussian (G^{++}, dashed lines). The distorted gaussian is parametrized as: $G^{++}(\xi; N, \bar{\xi}, \sigma, s, k) = \frac{N}{\sigma\sqrt{2\pi}} \exp\left(\frac{1}{8}k + \frac{1}{2}s\delta - \frac{1}{4}(2+k)\delta^2 + \frac{1}{6}s\delta^3 + \frac{1}{24}k\delta^4\right)$; where $\delta = (\xi - \bar{\xi})/\sigma$, $\bar{\xi}$ is the mean of the ξ distribution, σ is the square root of its variance, s is the skewness and k the kurtosis.

with best to date accuracy.

Preliminary measurements of the inclusive hadronic production cross sections have been performed at $BABAR$ with precision comparable to the previous measurements at ~ 91 GeV. These data will be very valuable for a better comprehension of the fragmentation process and in particular to study the scaling properties down to an energy of 10 GeV. The observed discrepancy between data and Monte Carlo predictions on scaling violation for etas, kaons and above all protons gives important experimental inputs for tuning models.

References

1. A.B. Arbuzov *et al*, *JHEP* **9812**, 009 (1998).
2. S. Binner, J.H. Kuhen and K. Melnikov, *Phys. Lett.* B **459**, 279 (1999).
3. M. Benayoun *et al*, *Mod. Phys. Lett.* A **14**, 2605 (1999).
4. B. Aubert *et al*, *BABAR* Collaboration, *Nucl. Instrum. Methods* A **479**, 1 (2002).
5. R.R. Akhmetshin *et al*, CMD-2 Collabration, *Phys. Lett.* B **466**, 392 (1999), *Phys. Lett.* B **475**, 190 (2000).
6. M.N. Achasov *et al*, SND Collaboration, *J. of Exp. and Theor. Physics* **96**, 789 (2003).
7. M. Davier, hep-ex/0312063 (2003).
8. M. Davier, S. Eidelman, A. Hoecker and Z. Zhang, *Eur. Phys. J.* C **31**, 503 (2003).
9. B. Aubert *et al*, *BABAR* Collaboration, Phys. Rev.**D-RC** 011103(R)(2004).
10. K. Hagiwara *et al*, Review of Particle Physics, *Phys. Rev.* D **66**, 010001 (2002).
11. W. Braunschweig *et al*, TASSO Collaboration, *Z. Phys.* C **42**, 189 (1989).
12. K. Abe *et al*, SLD Collaboration, *Phys. Rev.* D **59**, 052001 (1999).
13. T. Sjostrand, *Comput. Phys. Commun.* **82**, 74 (1994).
14. Y.I. Azimov, Y.L. Dokshitzer, V.A. Khoze and S.I. troian, *Z. Phys.* C **27**, 65 (1985).